Deuteration Effects on the in Vivo EPR Spectrum of the Reduced Secondary Photosystem I Electron Acceptor A_1 in Cyanobacteria†

Christof Klughammer,*,‡ Barbara Klughammer,‡ and Ron Pace§

Lehrstuhl für Botanik I, Julius-von-Sachs Institut für Biowissenschaften, Universität Würzburg, Julius-von-Sachs Platz 2, D-97082 Würzburg, Germany, and Department of Chemistry, Faculty of Science, The Australian National University, Canberra ACT 0200, Australia

Received October 13, 1998; Revised Manuscript Received January 13, 1999

ABSTRACT: The photoreduction of the secondary PSI electron acceptor A_1 in vivo has recently been detected via X-band EPR spectroscopy in intact spinach chloroplasts and in marine cyanobacteria *Synechococcus* PCC 7002 [Klughammer, C., and Pace, R. J. (1997) *Biochim. Biophys. Acta 1318*, 133−144]. A further study of the A_1^- EPR spectrum of *Synechococcus* PCC 7002 at room temperature with higher-field resolution revealed partially resolved hyperfine structure which was dominated by 0.4 mT splittings of three equivalent protons. The hyperfine splitting was not significantly affected by incubation of the cyanobacteria in ^2H_2O medium for 20 h, but was absent in fully deuterated cyanobacteria that were grown in ^2H_2O medium. Anisotropic *g*-factors consistent with a phylloquinone radical were derived by spectra simulation. Biosynthetic protonation of quinones via the CH_3 donor L-methionine in deuterated cells maintained hyperfine structure in the A_1^- spectrum, indicating the incorporation of CH_3 groups in 60% of the deuterated, photoactive A_1 molecules. Conversely, biosynthetic quinone deuteration via L-[methyl-d_3]methionine in protonated cells led to the loss of the 0.4 mT splittings in 54% of the A_1 molecules. These observations confirm the conclusion of Heathcote et al. [(1996) *Biochemistry 35*, 6644−6650] of the identity of EPR-detected, photoreduced A_1^- in vivo with a phylloquinone (vitamin K_1) radical in PSI. The partially resolved hyperfine structure of the A_1^- spectrum indicates an altered spin distribution in the bound vitamin K_1^- radical in vivo compared to that of unbound vitamin K_1^- in vitro.

The reaction center of photosystem I in higher plants, algae, and cyanobacteria comprises a chain of six redox centers named P700,[1] A_0, A_1, F_X, F_A, and F_B (for reviews, see refs *1*−*3*). The primary donor P700 consists of a pair of chlorophyll *a* molecules which transfer excited electrons to the primary chlorophyll *a* acceptor A_0. F_X, F_A, and F_B are [4Fe-4S] clusters, with F_X accepting electrons from the secondary acceptor A_1 (*4*−*7*). The existence and identity of A_1 have been determined from the appearance of an asymmetric 10.5 G wide EPR spectrum centered at $g = 2.0051$ after illumination at 230 K of dithionite-reduced PSI particles (*8*), from P700 triplet formation yield and power saturation studies of EPR signals of PSI particles at similar conditions (*9*), and from the presence of two phylloquinone (vitamin K_1) molecules per P700 in the reaction center of PSI (*10*). Only one phylloquinone molecule seems to be involved in electron transfer (*11*). Further evidence for the identity of A_1 and vitamin K_1 came from recent ENDOR and special triple-resonance studies on PSI of spinach and cyanobacteria (*12*), from quinone depletion and replacement studies affecting the electron spin polarized EPR signal of PSI (*13*), and from a determination of the **g**-tensor of A_1 at Q-band (*14*). On the other hand, the assignment of the photoaccumulated A_1^- EPR spectrum to a phylloquinone radical has been challenged by a result of Barry et al. (*15*). A specific deuteration of the 2-methyl group of phylloquinone in *Anabaena* had no effect on the A_1^- EPR spectrum in isolated PSI, although this methyl group causes a 7 MHz splitting in the ENDOR spectrum of vitamin K_1 in vitro (*15*). In contrast, Heathcote et al. (*16*) did find a narrowing of the photoaccumulated signal with biosynthetic deuteration of phylloquinone in *Anabaena variabilis*. The discrepancy has been explained by differences in the PSI preparation, which may give rise to spurious signals at $g = 2$ (*16*). In fact, when different A_1^- spectra in the literature generated by photoaccumulation in frozen, prereduced PSI particles are compared (*8*, *15*, *17*−*22*), it seems that the shape of the spectrum is variable in showing more or less fine structure. One reason for the variability of the A_1^- EPR spectrum could be the temperature- and illumination time-dependent reduction of A_0, which can cause loss of resolution of the hyperfine lines from A_1^- (*22*).

In a recent study, we have shown that the A_1^- radical can accumulate under in vivo conditions when dark-adapted cells of *Synechococcus* PCC 7002 are illuminated by a saturating 500 ms light pulse (*23*). This in vivo measuring system allows a point by point accumulation of the spectrum of A_1^- for the study of the effect of biosynthetic deuteration on the

† This work was supported by the Deutsche Forschungsgemeinschaft and the Australian Research Council.

* To whom correspondence should be addressed.

‡ Universität Würzburg.

§ The Australian National University.

[1] Abbreviations: A_1, secondary electron acceptor in photosystem I; ENDOR, electron nuclear double resonance; EPR, electron paramagnetic resonance; P700, primary electron donor of photosystem I; PSI and -II, photosystem I and II, respectively.

10.1021/bi982431o CCC: $18.00
Published on Web 03/05/1999

in vivo A_1^- EPR spectrum. As will be shown in this article, the in vivo A_1^- EPR spectrum reveals partially resolved hyperfine structure when measured with sufficient magnetic field resolution (0.2 mT). The hyperfine structure was affected by complete deuteration of the organism as well as by specific, biosynthetic deuteration via L-[methyl-d_3]-methionine, but not by an incubation of the cells in ^2H_2O for 20 h. Results from an inverse experiment will also be presented, in which hyperfine structure could be maintained by biosynthetic protonation of deuterated cells via L-methionine.

MATERIALS AND METHODS

Protonated cells of *Synechococcus* PCC 7002 were grown in standard medium as described in ref *24* and concentrated via centrifugation to yield a chlorophyll concentration of 0.83 mg/mL. ^2H_2O washing was performed by resuspending the cells in ^2H_2O medium. The concentration was 95 at. % ^2H after resuspension. The cells were kept in the dark for 20 h and concentrated to a final chlorophyll concentration of 0.50 mg/mL.

Fully deuterated cells of *Synechococcus* PCC 7002 were grown in ^2H_2O medium which was prepared like the standard medium by using ^2H_2O (99.7%) instead of H_2O. The final ^2H concentration was >99 at. %. For EPR measurements, the cells were concentrated to a final chlorophyll concentration of 0.21 mg/mL.

Biosynthetic incorporation of methyl groups in deuterated cells was achieved by growing *Synechococcus* PCC 7002 in ^2H_2O medium (>99 at. % ^2H) containing 1 mM L-methionine. A final chlorophyll concentration of 0.23 mg/mL was used for EPR measurements.

Biosynthetic incorporation of C^2H_3 groups in protonated cells was achieved by growing *Synechococcus* PCC 7002 in standard medium containing 6.5 mM L-[methyl-d_3]methionine (C/D/N Isotopes, Quebec, PQ). A final chlorophyll concentration of 0.65 mg/mL was used for EPR measurements.

All cells were cultivated under sterile conditions. After centrifugation, the cells were kept at room temperature in the dark for several hours to achieve stable anaerobic conditions.

EPR measurements were carried out at room temperature in the $g = 2$ region with a Bruker ESP 300 E X-band spectrometer, operating in the derivative mode at 9.79 GHz and equipped with a TM 110 resonator and a flat quarz cell (Wilmad Glass). The magnetic field was modulated with a frequency of 100 kHz and an amplitude of 0.2 mT. The microwave power was 50 mW. Time resolution was set on 10 ms. The microwave frequency was measured with the integrated frequency counter of the Bruker microwave bridge ER041XK, and the magnetic field was calibrated with a standard sample of DPPH (1,1-diphenyl-2-picrylhydrazyl radical; $g = 2.0036$). The sample was illuminated with white light of a xenon lamp (150 W) equipped with a Balzers DT Cyan dichroic filter ($\lambda < 700$ nm) through a nonmagnetic fiberoptic light guide attached to the window of the resonator. The actinic light pulses with an intensity of 18 000 μE m^{-2} s^{-1} at the window of the resonator were switched on and off by a computer-controlled photoshutter (Uniblitz). A personal computer with a digitizer board (DASH-16, Metra Byte) was used for A/D conversion and data recording.

Spectra of light pulse-induced EPR changes were generated point by point as described previously (*23*). Six transients with 60 s dark intervals were averaged for one sample. The durations of the light pulses were adjusted between 500 and 800 ms to achieve steady state reduction of A_1 in the different samples as indicated in the figure legends. Signal II_{slow} (thyrosine Y_D^+) was measured by averaging 10 magnetic field scans on a sample in the dark after illumination for 15 s followed by a 5 min dark period.

The X-band A_1^- EPR spectra were simulated by assuming powder pattern spectra of randomly oriented radicals, *g*-anisotropy, anisotropic hyperfine couplings of three equivalent β-protons of a CH_3 group, and an additional isotropic Gaussian line broadening. At room temperature, a rapid rotation of the CH_3 group along the C−C bond axis can be assumed, justifying the assumption of a hyperfine tensor with axial symmetry along the C−C bond axis. In the phylloquinone molecule, the C−C bond axis of the 2-methyl group forms an angle of 60° with the molecular axis connecting the quinone oxygens. When a coordinate system with the molecular *x*-axis along the C−O bonds and the *z*-axis perpendicular to the ring system is chosen, the principal **g**-tensor values can be assigned to the molecular axes with $g_{xx} > g_{yy} > g_{zz}$ (*25*). Therefore, the axially symmetric hyperfine tensor ($A_{||}$, $A_\perp$) has been rotated around the *z*-axis by 60° to match the axes of the molecular **g**-axis frame. For calculation of powder pattern spectra, one octant of the unit sphere was divided into 1500 sectors of equal area as described in ref *26*. For each sector, the magnetic field values of microwave absorption were calculated and the relative absorption intensities of all sectores were integrated. The obtained absorption band was differentiated and compared with the measured spectra.

RESULTS

Partially Resolved Hyperfine Structure in the A_1^- EPR Spectrum in Vivo. Figure 1A shows kinetics and spectra of light-induced EPR absorption changes of dark-adapted cells of *Synechococcus* PCC 7002 in the $g = 2$ region at a resolution of 0.2 mT. As has been shown previously (*23*), the changes can be separated into two main components. The first component is caused by a rapid transient oxidation of the primary PSI donor, P700, during the first 100 ms of the illumination (signal I). A second component, which builds up with a lag phase of about 90 ms, has been identified with the reduction of the secondary PSI acceptor A_1. A spectrum taken from a time interval 30−37 ms after the onset of light exposure represents the symmetric and 0.73 mT wide signal I centered at $g = 2.0027$, and a second spectrum taken from an interval 300−500 ms after the onset of light exposure shows the EPR spectrum of A_1^- in vivo (Figure 1B). Interestingly, the light-induced spectrum of A_1^- not only appeared to be asymmetric but also revealed some structure which may be due to partially resolved proton hyperfine splitting. It should be mentioned that EPR spectra of very similar shape have been published of reduced A_1 measured at low temperatures in PSI particle preparations (e.g., Figure 4 in ref *17*). In fact, the presented A_1^- EPR spectrum can be simulated by assuming anisotropic *g*-factors similar to that of a semiquinone like vitamin K_1^- (Table 1), which have been accurately determined by W-band EPR in vitro (*25*),

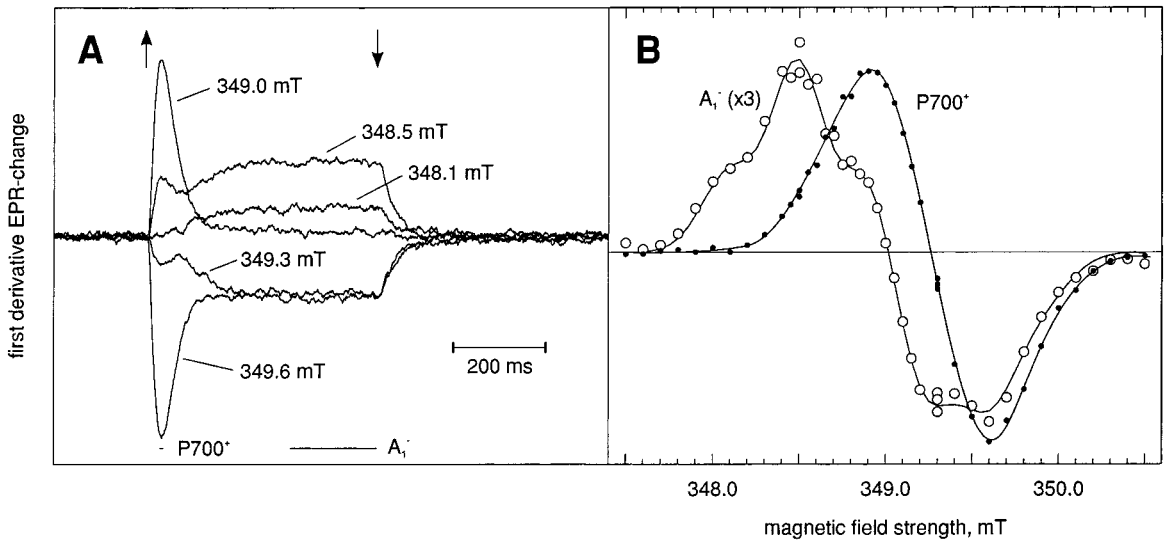

FIGURE 1: Time-resolved EPR spectral changes at $g = 2$ in dark-adapted, protonated cells of *Synechococcus* PCC 7002 (0.83 mg/mL) at room temperature induced by a 500 ms satutating light pulse (18 000 μE m^{-2} s^{-1}). (A) Kinetics at various magnetic field values. Up and down arrows indicate the onset and termination of the light pulse, respectively. The bottom lines indicate two time intervals centered at 33 and 407 ms after the onset of light exposure, from which the spectra of signal I ($P700^+$) and of A_1^- were plotted, respectively. (B) Light pulse-induced EPR spectra of $P700^+$ (●) and of A_1^- (○) observed 33 and 407 ms after the onset of light exposure, respectively. Note the 3-fold expanded scale for the A_1^- spectrum. The interconnecting line of the A_1^- spectrum represents a simulated powder pattern spectrum of a radical with *g*-anisotropy and with hyperfine coupling of three equivalent protons (parameters listed in Table 1). The following spectrometer settings were used: modulation amplitude, 0.2 mT; modulation frequency, 100 kHz; microwave power, 50 mW; time constant, 10 ms; and frequency, 9.790 GHz.

Table 1: *g*-Factors, Line Widths, and 2-Methyl Hyperfine Coupling Constants (hfcs) of the Vitamin K_1^- Radical in Vitro, of A_1^- at Low Temperatures, and of A_1^- in Vivo

		vitamin K_1	vitamin K_1	A_1^- *Synechocystis* PCC 6803	A_1^- *A. variabilis*/spinach	A_1^- *Synechococcus* PCC 7002 (room temperature) X-band EPR[a]			
		130 K W-band EPR (*25*)	60 K ENDOR (*12*)	20 K 283 GHz EPR (*22*)	60 K ENDOR (*12*)	protonated (Figure 1B)	protonated with d_3-methionine (Figure 4A)	deuterated (Figure 2B)	deuterated with methionine (Figure 4B)
g-factor	g_{xx}	2.0057	–	2.0063	–	2.0062	2.0061	2.0060	2.0062
	g_{yy}	2.0049	–	2.0050	–	2.0050	2.0051	2.0050	2.0051
	g_{zz}	2.0022	–	2.0023	–	2.0016	2.0022	2.0014	2.0023
line width (mT)	$\Delta B(g_{xx})$	0.84	–	–	–	0.38	0.38	0.22	0.20
	$\Delta B(g_{yy})$	0.82	–	–	–	0.38	0.38	0.35	0.20
	$\Delta B(g_{zz})$	0.92	–	–	–	0.38	0.38	0.50	0.20
2-methyl hfcs (mT)	$A_{\|\|}$	–	0.36[b]	–	0.46/0.45[b]	0.46	–	–	0.41
	$A_\perp$	–	0.24[b]	–	0.32/0.32[b]	0.32	–	–	0.29

[a] Accuracy of *g*-factors estimated to within 0.0002 and of hfcs within 0.02 mT. Accuracy may be less with contribution of another radical to the accumulated A_1^- spectra (see the text). [b] Calculated from ENDOR data via the equation $A(\text{mT}) = A(\text{MHz})/28$.

an anisotropic hyperfine coupling of three equivalent protons with axial symmetry (coupling constants $A_{||} = 0.46$ mT, $A_\perp = 0.32$ mT) and with a homogeneous Gaussean line width of 0.38 mT (Figure 1B). Hence, the spectrum is consistent with the identity of EPR-detected A_1^- in vivo with a vitamin K_1^- radical and implies that the shape of the spectrum is largely determined by the hyperfine coupling of the three β-protons of the 2-methyl group in vitamin K_1 (see Figure 5).

Effect of Deuteration on the A_1^- EPR Spectrum in Vivo. Figure 2A shows that cells of *Synechococcus* PCC 7002 grown in normal H_2O medium but washed and kept for 20 h in a medium containing 95% ^2H_2O display virtually the same spectra of signal I and of A_1^- as untreated cells. There may be minor changes in the shoulders of the maximum and in the minimum of the A_1^- spectrum, but the main shape of the spectrum does not seem to be significantly affected by the interaction of weakly bound, exchangeable protons. In contrast, the EPR spectra of fully deuterated cyanobacteria grown in ^2H_2O medium (>99% ^2H_2O) were remarkably altered (Figure 2B). Signal I was narrowed to a symmetrical, 0.35 mT wide signal, whereas the spectrum of A_1^- changed into a narrow (0.4 mT peak to peak) but asymmetric spectrum, indicating a large contribution of proton hyperfine splitting to the in vivo A_1^- EPR spectrum. The asymmetric shape of the A_1^- spectrum of the fully deuterated cyanobacteria may partially be due to the anisotropic **g**-tensor components known for vitamin K_1 (*25*), but the spectrum could not be simulated without the assumption of an extremely inhomogeneous line broadening and an unusually low g_{zz} value of 2.0014 (Table 1). Such a low g_{zz} value is not only different from the value of 2.0022 of vitamin K_1 (*25*), but it is also much lower than the value of 2.0023 obtained for A_1^- in *Synechocystis* membrane fragments at 283 GHz (*22*). Therefore, it is likely that in Figure 2B the true A_1^- spectrum has been distorted in the higher-field

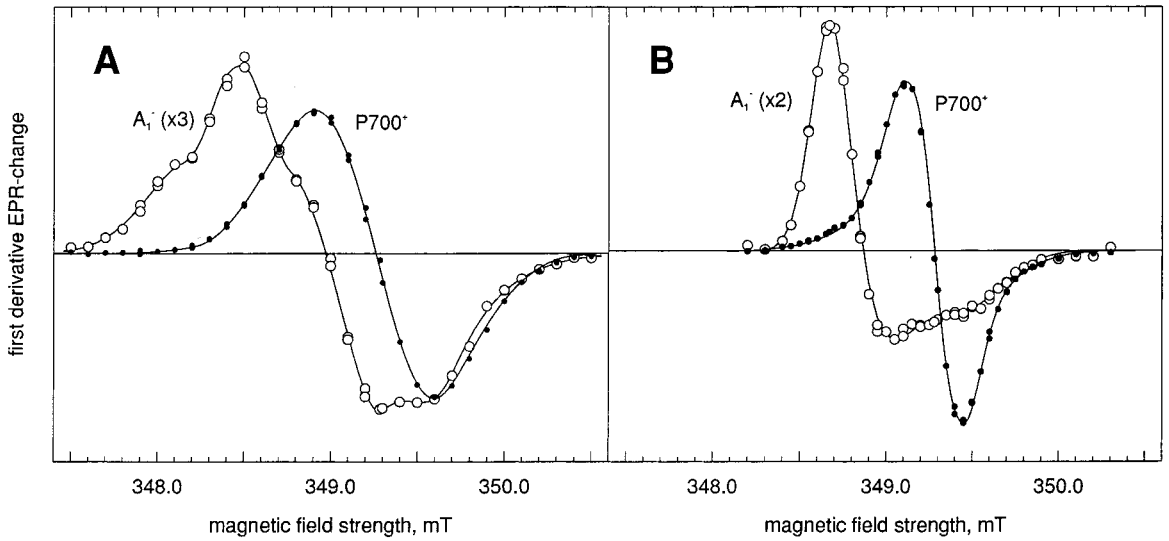

FIGURE 2: Effect of deuteration on the EPR spectra of $P700^+$ and A_1^- in *Synechococcus* PCC 7002 at $g = 2$. (A) Spectra of protonated cells (0.50 mg/mL) which have been incubated in ^2H_2O (95%) for 20 h induced by a 800 ms saturating light pulse (18 000 μE m^{-2} s^{-1}). The spectra of $P700^+$ (●) and of A_1^- (○) were plotted from data taken 46 and 740 ms after the onset of light exposure, respectively. Note the 3-fold expanded scale for the A_1^- spectrum. (B) Spectra of fully deuterated cells (0.21 mg/mL) induced by a 700 ms saturating light pulse (18 000 μE m^{-2} s^{-1}). The spectra of $P700^+$ (●) and of A_1^- (○) were plotted from data taken 70 and 670 ms after the onset of light exposure, respectively. Note the 2-fold expanded scale for the A_1^- spectrum. The interconnecting line of the A_1^- spectrum represents a simulated powder pattern spectrum of a radical with *g*-anisotropy and anisotropic line broadening (parameters listed in Table 1). The same spectrometer settings described in the legend of Figure 1 were used.

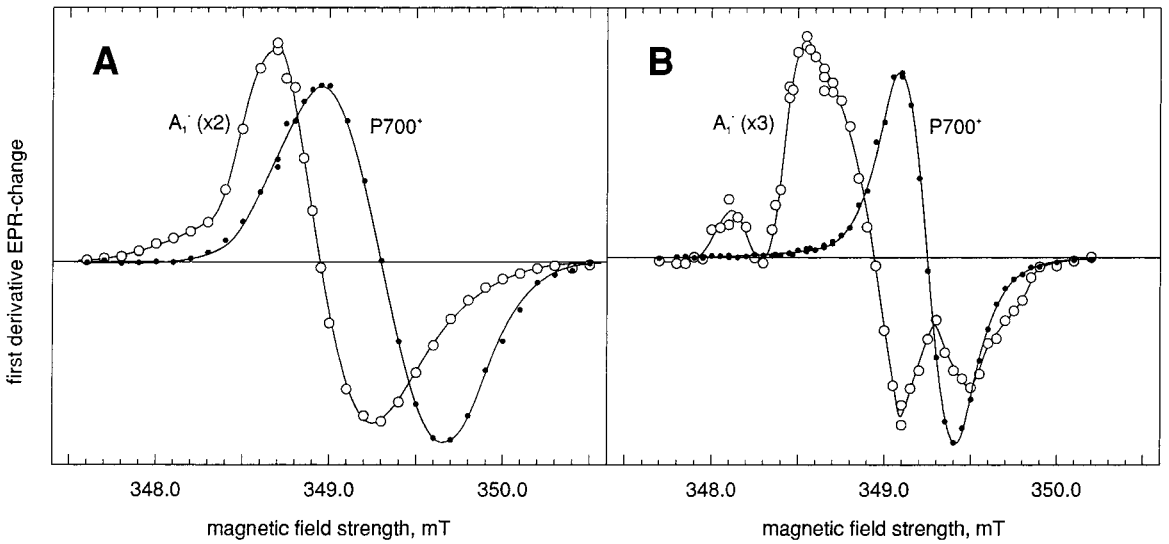

FIGURE 3: Effects of biosynthetic deuteration and biosynthetic protonation on the EPR spectra of $P700^+$ and A_1^- in *Synechococcus* PCC 7002 at $g = 2$. Reduction of A_1 was induced by 700 ms saturating light pulses (18 000 μE m^{-2} s^{-1}). (A) Spectra of protonated cells (0.65 mg/mL) grown in the presence of 6.5 mM L-[methyl-d_3]methionine. The spectra of $P700^+$ (●) and of A_1^- (○) were plotted from data taken 46 and 600 ms after the onset of light exposure, respectively. Note the 2-fold expanded scale for the A_1^- spectrum. The microwave frequency was 9.791 GHz. (B) Spectra of deuterated cells (0.23 mg/mL) grown in the presence of 99% ^2H_2O and 1 mM L-methionine. The spectra of $P700^+$ (●) and of A_1^- (○) were plotted from data taken 46 and 600 ms after the onset of light exposure, respectively. Note the 3-fold expanded scale for the A_1^- spectrum. The microwave frequency was 9.789 GHz. The other spectrometer settings were as described in the legend of Figure 1.

region by another light-generated radical species which could not be separated kinetically from the A_1 redox change and consequently has led to an incorrect determination of g_{zz}.

Effect of Biosynthetic Deuteration or Protonation on the A_1^- EPR Spectrum in Vivo. Simulation of the A_1^- EPR spectrum of Figure 1B was consistent with the 2-methyl group in vitamin K_1 being largely responsible for the partially resolved hyperfine structure. If this interpretation was correct, deuteration of the 2-methyl group should have a distinct effect on the spectrum. It was shown that methionine can be a CH_3 donor for phylloquinone and plastoquinone in cyanobacteria (*27*) and led to incorporation of methyl groups in methionine auxotrophs of *A. variabilis* (*15*, *16*).

Figure 3A shows EPR spectra of *Synechococcus* PCC 7002 cells which were fed 6.5 mM [methyl-d_3]methionine during growth. Although the experiment was carried out with wild type *Synechococcus* PCC 7002, the A_1^- spectrum was substantially narrowed (0.55 mT width) and had lost most of its hyperfine structure. However, the spectrum remained broader than that of the fully deuterated cyanobacteria (Figure 2B), which may partially be due to incomplete biosynthetic deuteration and partially due to line broadening caused by

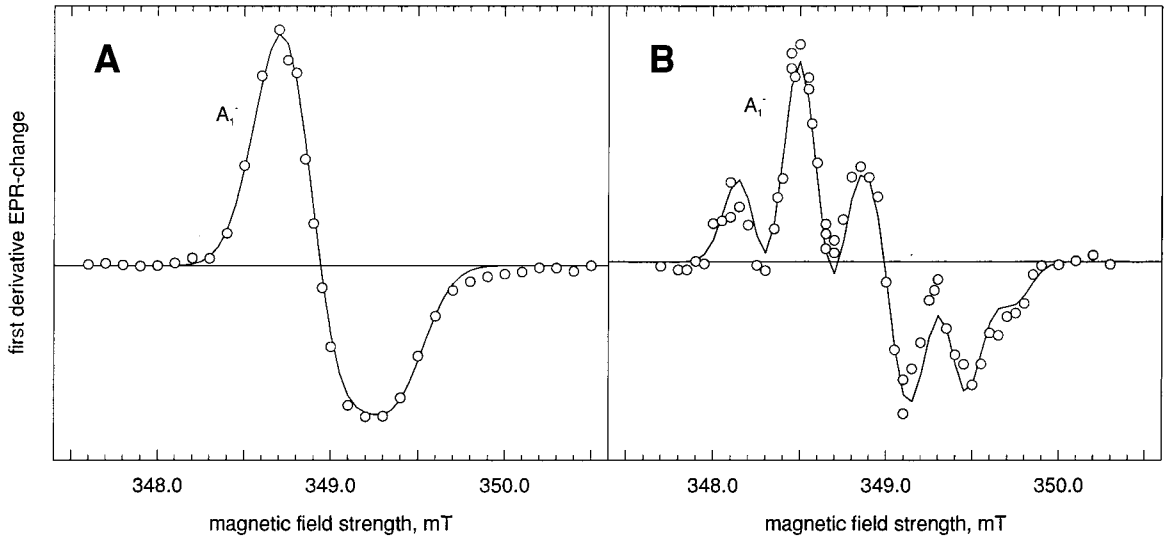

FIGURE 4: Deconvoluted and simulated A_1^- EPR spectra of biosynthetic deuterated and of biosynthetic protonated cells of *Synechococcus* PCC 7002 at $g = 2$. (A) A_1^- spectrum of Figure 3A corresponding to 54% of the doubly integrated amplitude after subtraction of the A_1^- spectrum of protonated cells (Figure 1B). The interconnecting line represents a simulated powder pattern spectrum of a radical with *g*-anisotropy and isotropic line broadening. (B) A_1^- spectrum of Figure 3B corresponding to 60% of the doubly integrated amplitude after subtraction of the A_1^- spectrum of deuterated cells (Figure 2B). The interconnecting line represents a simulated powder pattern spectrum of a radical with *g*-anisotropy and with hyperfine coupling of three equivalent protons. Simulation parameters are listed in Table 1.

hyperfine interaction of the remaining protons within the vitamin K_1 molecule. In contrast to the spectrum of A_1^-, the spectra of signal I (Figure 3A) and of signal II_{slow} (not shown) were not affected by the incorporation of deuterated methyl groups.

The responsibility of the methyl group in vitamin K_1 for most of the hyperfine structure of the A_1^- spectrum was further confirmed by an inverse experiment in which the cyanobacteria were grown in a medium containing 99% ^2H_2O and fed protonated methionine (1 mM). Figure 3B shows that in these cells hyperfine structure in the A_1^- spectrum was present to an appreciable extent. As expected, the structure was even better resolved than in protonated cyanobacteria in which the weakly interacting protons obviously have broadened and thereby obscured the hyperfine pattern of the methyl group in vitamin K_1. However, the A_1^- spectrum of the biosynthetically protonated cyanobacteria (Figure 3B) does not resemble the A_1^- spectrum of the protonated cyanobacteria (Figure 1B) with narrowed hyperfine lines. This is because the A_1^- spectrum of Figure 3B has to be considered a mixture of two spectra: one generated by acceptors A_1 with incorporated CH_3 groups and another generated by the unaffected, fully deuterated A_1^- molecules. As with the protonated cyanobacteria, both signal I (Figure 3B) and signal II_{slow} (not shown) remained narrow and completely unaffected by biosynthetic input of methyl groups during methionine feeding of the cells.

The deconvoluted A_1^- spectrum of protonated cells having C^2H_3 groups incorporated into all A_1 molecules may be obtained from the A_1^- data shown in Figure 3A by subtracting an appropriate amplitude of the native A_1^- spectrum of Figure 1B. Analogously, the A_1^- spectrum of deuterated cells having CH_3 groups incorporated into all A_1 molecules may be obtained from the data of Figure 3B by subtraction of an appropriate amplitude of the spectrum of fully deuterated cells (Figure 2B). As the subtraction amplitudes are not known, they have to be properly adjusted to yield reasonable results (Figure 4). With the chosen amplitudes, the efficiencies of C^2H_3 group incorporation and of CH_3 group incorporation were quantified by the ratios of the corresponding doubly integrated A_1^- spectra of Figures 3 and 4 to 54 and 60%, respectively.

The spectrum in Figure 4A, which represents the deconvoluted A_1^- spectrum of protonated cyanobacteria with incorporated C^2H_3 groups, can be satisfactorily simulated with similar parameters for *g*-factors and line widths as used for the spectrum of fully protonated cells but by omitting hyperfine splitting of the three methyl protons (Table 1). Vice versa, the spectrum in Figure 4B, representing the deconvoluted A_1^- spectrum of deuterated cyanobacteria with incorporated CH_3 groups, can be simulated well with *g*-factors similar to those of normal protonated cells, but with a narrow homogeneous line width (0.2 mT) and with the axial symmetric hyperfine constants of the three equivalent methyl protons ($A_{||} = 0.41$ mT, $A_{\perp} = 0.29$ mT) which are slightly smaller than those used for the fully protonated cells (Table 1).

DISCUSSION

We have shown that under in vivo conditions at room temperature the light-induced A_1^- EPR spectrum of *Synechococcus* PCC 7002 reveals partially resolved hyperfine structure at a magnetic field resolution of 0.2 mT. A very similar hyperfine pattern can be observed with isolated chloroplasts of spinach at room temperature (data not shown). Modeling of the powder pattern spectrum implies the dominance of three equivalent protons which are coupled to the unpaired spin of the radical with axially symmetric hyperfine coupling constants $A_{||}$ of 0.46 mT and $A_{\perp}$ of 0.32 mT. Almost identical hyperfine coupling constants were recently determined by ENDOR and special triple resonance for the photoaccumulated A_1^- in photosystem I particles of *A. variabilis* and of spinach at 60 K and have been assigned to the 2-methyl group of phylloquinone (*12*). This is consistent with the observation that a 20 h incubation period

for the cells in ^2H_2O did not alter the overall hyperfine pattern. Small differences between the spectra of fully protonated and ^2H_2O-incubated cells may be within the error of spectrum acquisition and are presumably not significant. Also, the weaker coupled protons of the A_1 molecule, which cause line broadening rather than contribute to the hyperfine pattern, seem not to be affected by proton exchange. As expected, the hyperfine pattern was absent and the line width was substantially narrowed in the fully deuterated cyanobacteria. However, the true A_1^- spectrum may have been distorted by the superimposed spectrum of another light-induced radical in the higher-field region, leading to an incorrect determination of g_{zz} by simulating the spectrum. Since the contribution of another radical also cannot be excluded for the other accumulated A_1^- spectra, this may put a general limit on the accuracy of the calculated *g*-values and hyperfine constants. The involvement of $P700^+$ as a simple explanation is unlikely as the *g*-value of the radical would have to be approximately 2.0014, significantly lower than that of $P700^+$ (2.0027). Also for the normal protonated cyanobacteria, a rather low g_{zz} of 2.0016 was the best value for simulation of the A_1^- spectrum, whereas for the spectra displayed in panels A and B of Figure 4, g_{zz} values closer to that of isolated vitamin K_1 were determined. While an accurate determination of g_{zz} seems to be difficult by simulation of the accumulated spectra, the values of g_{xx} and g_{yy} did exhibit little variation and seem to be shifted slightly positive compared to those of isolated vitamin K_1 (Table 1).

In further experiments, the hyperfine pattern, but not the line width, was found to be highly sensitive to biosynthetic incorporation of CH_3 groups into the quinone synthesis pathway via methionine. It was found that the hyperfine pattern can be abolished in protonated wild type cells in about 54% of the light reducible A_1 by feeding the cells the C^2H_3 donor [methyl-d_3]methionine (6.5 mM). By feeding the CH_3 donor methionine (1 mM) to cells grown in ^2H_2O, we were able to detect hyperfine splitting in about 60% of the light reducible A_1. Although considerably high concentrations of methionine were used, in both experiments only about half-complete incorporation could be achieved, indicating a principal limit for the competitive input of externally added methionine during quinone synthesis in wild type cyanobacteria.

Since methionine has been shown to act as a methyl group donor in the pathway of quinone synthesis (*27*), it is reasonable to conclude that the three protons giving rise to the hyperfine structure in the A_1^- EPR spectrum are identical to the β-protons of a rotating CH_3 group located at the ring system of a quinone molecule. Consequently, the responsible methyl group may be identified with the 2-methyl group of phylloquinone (Figure 5) which has been shown to be a component of the PSI reaction center (*10*). Hence, the component giving rise to the in vivo A_1^- EPR spectrum is definitely identical with a phylloquinone molecule (vitamin K_1).

The spectra in Figures 1B and 4B indicate average coupling constants of 0.37 and 0.33 mT for the β-protons at position 2 of phylloquinone, respectively. At present, we do not know whether the difference of 0.04 mT is significant and indicates a slightly decreased spin density on C_2 of vitamin K_1 in deuterated cells. However, for the isolated phylloquinone radical, in vitro splittings of 7 MHz (*15*) and

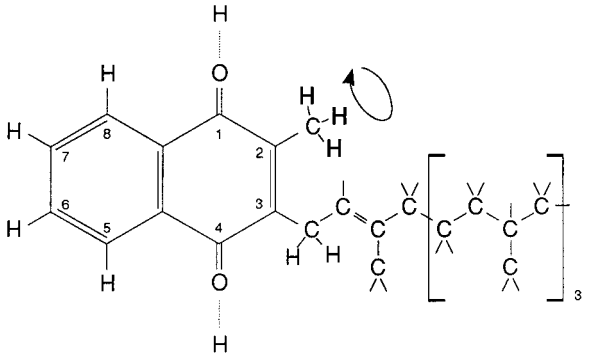

FIGURE 5: Chemical structure of 2-methyl-3-phytyl-1,4-naphthoquinone (vitamin K_1). Only those protons which presumably affect the EPR spectrum of the radical are depicted. The data provide evidence that the partially resolved hyperfine structure in the A_1^- EPR spectrum in vivo is caused by the three protons of the rotating 2-methyl group (bold letters).

7.9 MHz (*12*) for the 2-methyl group were determined by ENDOR, equivalent to hyperfine coupling constants of 0.26 and 0.28 mT, respectively, significantly lower than the values described above. Very similar coupling constants for the β-protons at C_2 have been reported in ref *28*. Hence, the spin density must be significantly increased by about 30−40% at position 2 of phylloquinone in PSI compared to that of the unbound radical, because the hyperfine splitting is proportional to the spin density at the corresponding ring carbon atom of the molecule (*29*). In this context, it may be noted that a spin density increase of 31% for the same site has been calculated from recent results of ENDOR and special triple resonance measurements on *A. variabilis*, which has been interpreted by the influence of the protein environment of A_1 (*12*). In addition to this, the coulomb field of a negative charge on the nearby located, reduced acceptor F_X may have an influence on the spin distribution within the A_1^- molecule. This may be seen when hyperfine constants obtained from room-temperature electron spin polarized signals (oxidized F_X) are compared with room-temperature data of photoreduced A_1 (reduced F_X) presented here. More precise *g*-factors and hyperfine constants could be obtained with complete labeled phylloquinone in PSI which may be achieved with a methionine auxotroph mutant such as Met-27 of *A. variabilis* (*16*).

ACKNOWLEDGMENT

Dr. Karin Ahrling is thanked for fruitful discussions and for support in EPR simulations. Dr. Murray Badger (Research School of Biological Sciences, The Australian National University) is thanked for his cooperation and for providing facilities for cultivation of the cyanobacteria.

REFERENCES

1. Golbeck, J. H., and Bryant, D. A. (1991) in *Current Topics in Bioenergetics* (Govindjee, Ed.) pp 83−177, Academic Press, London.
2. Golbeck, J. H. (1995) in *The Molecular Biology of Cyanobacteria* (Bryant, D. A., Ed.) pp 319−360, Kluwer Academic Publishers, Dordrecht, The Netherlands.
3. Brettel, K. (1997) *Biochim. Biophys. Acta 1318*, 322−373.
4. Brettel, K. (1988) *FEBS Lett. 239*, 93−98.
5. Lüneberg, J., Fromme, P., Jekow, P., and Schlodder, E. (1994) *FEBS Lett. 338*, 197−202.

6. Moënne-Loccoz, P., Heathcote, P., Maclachlan, D. J., Berry, M. C., Davis, I. H., and Evans, M. C. W. (1994) *Biochemistry 33*, 10037−10042.
7. Van der Est, A., Bock, C., Golbeck, J., Brettel, K., Sétif, P., and Stehlik, D. (1994) *Biochemistry 33*, 11789−11797.
8. Bonnerjea, J., and Evans, M. C. W. (1982) *FEBS Lett. 148*, 313−316.
9. Gast, P., Swarthoff, T., Ebskamp, F. C. R., and Hoff, A. J. (1983) *Biochim. Biophys. Acta 722*, 163−175.
10. Schoeder, H.-U., and Lockau, W. (1986) *FEBS Lett. 199*, 23−27.
11. Schwartz, T., and Brettel, K. (1995) in *Photosynthesis: from Light to Biosphere* (Mathis, P., Ed.) Vol. II, pp 43−46, Kluwer Academic Publishers, Dordrecht, The Netherlands.
12. Rigby, S. E. J., Evans, M. C. W., and Heathcote, P. (1996) *Biochemistry 35*, 6651−6656.
13. Rustandi, R. R., Snyder, S. W., Biggins, J., Norris, J. R., and Thurnauer, M. C. (1992) *Biochim. Biophys. Acta 1101*, 311−320.
14. Thurnauer, M. C., Brown, J. W., Gast, P., and Feezel, L. L. (1989) *Radiat. Phys. Chem. 34*, 647−651.
15. Barry, B. A., Bender, C. J., McIntosh, L., Ferguson-Miller, S., and Babcock, G. T. (1988) *Isr. J. Chem. 28*, 129−132.
16. Heathcote, P., Moënne-Loccoz, P., Rigby, S. E. J., and Evans, M. C. W. (1996) *Biochemistry 35*, 6644−6650.
17. Heathcote, P., and Evans, M. C. W. (1980) *FEBS Lett. 111*, 381−385.
18. Mansfield, R. W., and Evans, M. C. W. (1986) *FEBS Lett. 203*, 225−229.
19. Mansfield, R. W., and Evans, M. C. W. (1988) *Isr. J. Chem. 28*, 97−102.
20. Ziegler, K., Maldener, I., and Lockau, W. (1989) *Z. Naturforsch. 44c*, 468−472.
21. Heathcote, P., Hanley, J. A., and Evans, M. C. W. (1993) *Biochim. Biophys. Acta 1144*, 54−61.
22. MacMillan, F., Hanley, J., van der Weerd, L., Knüpling, M., Un, S., and Rutherford, A. W. (1997) *Biochemistry 36*, 9297−9303.
23. Klughammer, C., and Pace, R. J. (1997) *Biochim. Biophys. Acta 1318*, 133−144.
24. Sültemeyer, D., Price, G. D., Yu, J. W., and Badger, M. R. (1996) *Planta 197* (4), 597−607.
25. Burghaus, O., Plato, M., Rohrer, M., Möbius, K., MacMillan, F., and Lubitz, W. (1993) *J. Phys. Chem. 97*, 7639−7647.
26. Åhrling, K. A., and Pace, R. J. (1995) *Biophys. J. 68*, 2081−2096.
27. Barry, B. A., and Babcock, G. T. (1987) *Proc. Natl. Acad. Sci. U.S.A. 84*, 7099−7103.
28. Das, M. R., Connor, H. D., Leniart, D. S., and Freed, J. H. (1970) *J. Am. Chem. Soc. 98*, 2258−2268.
29. McConnel, H. M. (1956) *J. Chem. Phys. 24*, 764.

BI982431O